Proceedings World Geothermal Congress 2020+1
Reykjavik, Iceland, April - October 2021

Statistical Model for Thinning Rates of Two-Phase Wells in Leyte Geothermal Production Field

Anthony S. Ponce

Energy Development Corporation, 38/F One Corporate Centre, Julia Vargas corner Meralco Avenue, Ortigas Center, Pasig City 1605 Philippines

ponce.as@energy.com.ph

Keywords: Geothermal, Leyte, Caliper, Thinning Rate, Philippines

ABSTRACT

Corrosion due to exposure to geothermal fluids is one of the technological problems faced by the geothermal industry. The flow of geothermal fluid causes deterioration of equipment due to corrosion and erosion; thus monitoring of facilities that come into contact with the fluid is vital to minimizing safety and environmental risks during geothermal operation. Since the geothermal well delivers two-phase fluid from the reservoir to the surface, its casing is the first equipment on the field that encounters the fluid. Corrosion and erosion reduce the casings' integrity by general corrosion (i.e. thinning) or localized attacks (e.g. pitting, cracking etc.). Caliper surveys may be conducted to monitor the thickness of well casings and detect pits on the casing inner wall that may eventually become holes. Effective management of the effects of corrosion requires a good understanding of how different corrosion factors contribute to the overall casing degradation. In this paper, statistical methods were used to explore the contribution of factors such as temperature, flow velocity, pH, well geometry, and corrosion species to the overall thinning rate of a geothermal casing. Downhole fluid chemistry of the wells were projected from the measured wellhead chemistry using chemical speciation software. Physical flow parameters, on the other hand, were simulated from measured wellhead conditions using wellbore modeling software. Linear regression models were built to correlate data estimated thinning rates used of two-phase production wells of the Leyte Geothermal Production Field (LGPF) with different factors affecting corrosion rate. Regression results were analyzed statistically using ANOVA, p-value test, and multiple regression coefficients. Adjusted R^2 of the regression analysis and mean absolute percentage error (MAPE) were used in selecting good regression models. The objectives are to determine which of the factors affecting casing thinning rate are most significant and eventually, predict the thinning rate of the casing based on surface measurements and known well data. The data can then be used to aid in the prioritization of wells lined up for caliper surveys.

1. INTRODUCTION

The objective of this study is to determine the significant factors and corrosion species that predominantly affects the thinning rate of the production casing and able to predict the thinning rate of the casing. This study is relevant in putting in place a systematic program for monitoring the casing condition of a geothermal well. This study aims to provide an idea on the average thinning rate of the casing using the simulated data from the sampled surfaced data sample of the well. The result of the study may also help to prioritize wells programmed for caliper measurements for monitoring the rate of corrosion in the well casings. The study will provide an industry update on the capability of existing tools for monitoring the corrosion of the casing both internal and external. The study is limited to two phase production wells of Leyte geothermal production field and it is concentrated only on the internal corrosion of the well.

After a geothermal production well was drilled and utilized to extract heat energy from a reservoir, certain problems occurs and one of these problems is corrosion, Casing corrosion, which is one of the challenging technological problems in managing a geothermal production field. Scaling is another technological problem during geothermal utilization.

Geothermal fluids contain CO_2, H_2S, NH_3 and chloride ions that can cause corrosion of metallic material. The fluid characteristics change over time as heat extraction takes place thus it is important to put in place a systematic procedure for the monitoring of the chemistry of the fluid from every geothermal well that is being utilized

The casings of a geothermal well are exposed to geothermal brine flow which causes thinning. The thinning of the casing, primarily as a result of material loss, compromises its integrity and this may eventually lead to casing breaks and casing collapse and consequently a reduction of well output. The casing breaks at shallow depths may cause steam to leak in the formation and within the pad. The steam leak within the overlap of the anchor casing and production casing may lead to an underground blowout. The high risk involved with an unreliable casing condition needs a systematic process of monitoring of casing integrity. This is for environmental and safety concerns and to ensure continuous geothermal well operation. The integrity of the casing is inspected using downhole logging tools such as caliper tools, electromagnetic tools, acoustic tools or video cameras; these tools are used to examine the condition of the casing.

Furthermore, the casing conditions of the production wells the Leyte geothermal production field are checked with casing inspection caliper surveys. In the Mahanagdong sector, the brine produced from the production wells have acidic pH or pH (25C) below 4.5 hence the casing of the wells were periodically checked using caliper surveys to monitor the thinning of the casing. One of the production wells in Mahanagdong area was plugged and abandoned after several years of utilization due to severe corrosion.

The high enthalpy single-phase steam-dominated wells of the Leyte geothermal production field were also monitored with caliper measurements. There is severe corrosion in these wells because of the presence of high quantity of suspended solids. The results of the caliper surveys served as a baseline for well utilization and intervention strategies in order to mitigate further deterioration of the casing.

The data from the caliper surveys of production wells in Leyte geothermal production field were used in the study of thinning rates of casing. The characteristic of the fluid discharge, such as fluid velocity, temperature, pH, fluid chemistry concentration, were used for studying the effects of the thinning rate on the casing.

2. CORROSION IN GEOTHERMAL WELLS

In a geothermal environment, the corrosion process depends on the chemical composition of the geothermal fluid or brine. The geothermal brine has a wide range of composition; from strongly acidic brine that corrode most common alloys to the more usual neutral pH waters that may lay protective scales on the metal surface. (Elguedri, 1999)

In a high-temperature geothermal field, the brine flashes inside the wellbore and changes from single- phase to two-phase due to the drop in pressure while the well is being flowed. Wahl (1977) discussed the effect of flashing on brine composition as the geothermal well produce steam. The flashing of the brine causes two main changes on the chemical concentration. First, by evaporating some of the water in the brine, a higher concentration of the remaining components is achieved while the brine is flashed to a sufficiently low pressure. The ratio of the brine between after flashing and before flashing is dependent on the weight fraction of water flashed. Second is the effect of flashing on the chemistry of the brine. Flashing removes certain constituents such as carbon dioxide or hydrogen sulphide. In most cases, carbon dioxide is the dominating gas in the fluid mix, this will have the most significant effect on the chemistry of the fluid. The effect of CO2 release in principle is the change in fluid pH. The next most significant is the reduction of dissolved CO_2 in the brine. When CO_2 dissolved in water, a small portion of it reacts chemically with H_2O to form carbonic acid. In water carbonic acid dissociates rapidly to form H+ ion and HCO_2 so it affects the carbonate equilibrium and pH values change as a result. The release of CO_2 from the solution will result to release of carbonate ion causing the pH of the fluid to increase.

2.1 Corrosion species in geothermal brine

There are key chemical species that produce significant corrosion effect on metallic materials. Conover, et al., (1979) generalized the corrosive effects of these chemical species.

- Hydrogen Ion (H^+). Increasing concentration of hydrogen (decrease in pH) will result in an increase in the rate of general corrosion for carbon steel especially when fluid has a pH below 7. The metal in fluid with higher than pH 7, (low concentration of hydrogen ion) forms a protective layer or film which minimizes the corrosion rate. However when the protective layer is broken, serious localized corrosion attack occurs which can cause pitting, crevice corrosion and stress corrosion cracking.

- Chloride Ion (Cl^-) – The chloride ion causes the local breakdown of passive films that protects the metal from uniform corrosion attack thus resulting in pitting, crevice corrosion, or stress corrosion cracking. The increase in chloride concentration can lead also to an increase in uniform corrosion but not as critical compared to the localized effect.

- Hydrogen sulphide (H_2S) – This corrosion specie is more severe for copper and nickel alloy. The effect of H_2S on iron-based materials is less predictable. It accelerates corrosion on the metal, but in some cases, it inhibits corrosion. High strength steels are often subject to sulphide stress cracking which is a form of hydrogen embrittlement. The oxidation of hydrogen sulphide in aerated geothermal process streams increases the acidity of the stream. A low concentration of hydrogen sulphide may have serious detrimental effects especially when oxygen is present.

- Carbon dioxide (CO_2) – In the acidic region, i.e. as in carbonic acid (H_2CO_3), it can accelerate the uniform corrosion of carbon steel. The pH of geothermal fluids and process streams is largely controlled by carbon dioxide. Carbonates and bicarbonates can display mild inhibitive effects.

- Ammonia (NH_3) – It can cause stress corrosion cracking of copper alloys and accelerate uniform corrosion in mild steels.

- Sulphate (SO_4-) – It plays a minor role in most geothermal fluids. However, in low chloride fluids, sulphate becomes the main aggressive anion; it rarely causes the same severity of the localized corrosion attack as chloride ion.

- Oxygen – Oxygen is present in low concentration in geothermal brine. Inadvertent intrusion of even traces of this gas into geothermal brine has led to serious accelerated corrosion. The addition of minor quantities of oxygen to a geothermal system can increase the chance of severe localized corrosion of normally resistant alloys. The corrosion of carbon steels is sensitive to trace amounts of oxygen.

- Transition metal ions – Transition metal ions could also be included as key species. Some oxidized forms of transition metals (Fe3+, Cu2+ and others) are corrosive but these ions are present in the lowest oxidation state in geothermal fluids. When transition metals are exposed to oxygen by aeration or mixing with water of different quality, oxygen can convert Fe2+ to Fe3+ which is another reason for scrubbing oxygen from geothermal streams.

2.2 Corrosion types encountered in geothermal systems

There are several types of corrosion attacks found in equipment used in a geothermal environment (Conover, et al., 1979). Some of the main modes of corrosion that occur in geothermal are as follows:

- Uniform corrosion. It is a general overall attack on the metal surface. It is often promoted by chloride, carbon dioxide, oxygen or ammonia.

- Pitting. This is a type of corrosion attack that is localized which results in the development of small pits in the metal surface. Pits are associated with the breakage of the protective film in the surface of the metal. It is susceptible to the increase in chloride and hydrogen ion content of the fluid.

- Crevice corrosion. It is a localized corrosion attack similar to pitting corrosion. This depends on geometry and forms in the crevice of the equipment.

- Stress corrosion cracking. This is a catastrophic type of failure promoted by a combination of tensile stress and the presence of chloride in the environment. Severity of the stress corrosion cracking increases when process happens with increasing temperature and in the presence of oxygen.

- Sulphide stress cracking. Similar to stress corrosion cracking, sulphide stress cracking is also a catastrophic type failure that results from exposure under stress of susceptible materials to a hydrogen sulfide environment in an aqueous phase. Contrary to the stress corrosion cracking, sulphide stress cracking decreases in severity with increasing temperature but low pH may greatly accelerate failure.

- Hydrogen blistering. This is the rupture of metallic material when hydrogen is trapped in voids and accumulates at a sufficient pressure. This occurs in low strength alloy steel in aqueous solutions containing hydrogen sulfide. The material need not be stressed for hydrogen blistering to occur.

- Intergranular corrosion. A regional corrosion that occurs around the grain boundaries or in the neighbour grains of metallic materials with little or no attack on the bodies of the grains. The alloy disintegrates or loses its strength or both.

- Galvanic corrosion. It occurs by electrical conduction of two different metals. The corrosion of a less noble material is accelerated in this kind of corrosion. During material selection, the order of the galvanic series is used as a reference for preventing galvanic corrosion.

- Fatigue corrosion. This is a premature fracture due to fluctuating stress exposed in a corrosive environment. Fatigue corrosion limit is the largest stress applied under a given condition of stress, temperature, and corrosive environment without causing the material to fail for a given number of cycles.

- Erosion-corrosion. It is the accelerated corrosion of one metal exposed to a corrosive fluid. This occurs when fluid flows faster than the critical velocity familiar to that metal. It is the abrasion of the metallic material by the striking of high velocity fluids to the hanging solid materials or particles. The metal that is exposed to this kind of corrosion does not form corrosion product on its surface.

2.3 Other factors affecting corrosion rate

Besides the chemical species present in geothermal fluid that significantly affect the corrosion rate of the metal, there are other factors that affect the corrosion rate. Some of the other factors of thinning rate are related to erosion-corrosion types where the fluid is exposed to the metallic material and damages the protective film created from its initial corrosion reaction. These factors are related to hydrodynamic parameters such as the temperature, pH, fluid velocity, two-phase flow quality, geometry of the flow, and pipe material component which influence the erosion-corrosion mechanism (Petric and Ksiazek, 1997). Several studies and laboratory experiments were conducted on the effect of environmental factors on corrosion of materials.

Effect of pH. Low pH affects the uniform corrosion rate of low carbon and low alloyed steels. According to Ikeuchi et al. (1982) the corrosion rate of a material is: a) inversely proportional to pH when the pH is in the range of 1 to 4 due to the active dissolution of materials; and b) is independent of pH when pH is in the range of 4 to 10. In flow accelerated corrosion, as the hot pH in the system become more acidic, the relative rate increases. The influence of pH in the erosion-corrosion is more serious than corrosion alone.

Effect of velocity. According to Sanada et al. (1998) corrosion rate is independent of flow rate when the flowrate ranges from 70 to 100 m/s. Meanwhile, for the erosion rate as the velocity increases, the corrosion rate increases. When the velocity comes close to the sound velocity, the material is damaged remarkably by cavitation-erosion (Ikeuchi et al., 1982)

Effect of temperature. Corrosion rates are significantly dependent on temperature (Sanada et al., 1998). The effect of temperature is high for alloys that have intermediate performance. However, the pH still has the dominant effect on the corrosion rate.

Effect of pipe geometry. Shape and size of a piping geometry has a significant impact on the flow-accelerated corrosion. This factor affects localized velocities and turbulence within the pipe component. A complex geometry could increase the localized velocity in a given section area by two to three times compared to the bulk velocity. (Petric and Ksiazek, 1997).

Effect of fluid quality. In a two-phase flow, the fluid flows along the wall of pipe. The temperature and pressure determine the amount of steam according to the mass fraction of the quality of the water/steam mixture. The steam quality determines the distribution of the voids within the flow stream which in turn affects the mass transfer and rate of the flow-accelerated corrosion.

Effect of metal alloy content. The amount of alloying material present in the metal affects the stability and solubility of the oxide layer on the surface. Traces of molybdenum, copper and particular chromium can have a significant impact on the rate of corrosion.

The influence of pH on the corrosion rate in two-phase fluid shows a dependence of material composition on the performance as shown in the experiment by Sanada et al., (1995) wherein carbon and low alloy steels were found to be severely corroded at a pH less than 3.5.

3. GEOCHEMISTRY OF THE PHILIPPINE GEOTHERMAL FIELDS

The dowhnole pH and sulphur chemistry as a function of boiling point temperatures were determined for a number of wells from different fields and these could be linked to the sulphide mineralogy of rocks recovered from the acid Cl-SO_4 wells (Lichti *et al.,* 1998). The produced fluids are classified into three types: low Cl, high SO4 with NA+K>Cl; high Cl, high SO_4 with CL>Na+K; and high Cl, high SO_4 with Na+K>Cl.

The Leyte geothermal production field in North Central Leyte is the largest geothermal area in the Philippines. It is a liquid-dominated high temperature geothermal field and its brine has neutral to low pH. The brine from the Mahanagdong sector of the Leyte geothermal production field has a pH (25C) ranging from 3 to 8 based on actual samples taken from the wells. It is inferred that the temperature of the aquifers in Mahanagdong ranges from 250 to 300°C and has higher concentrations of H_2S and H_2 in the initial aquifer fluids, which are assumed to be purely liquid, than those at the equilibrium with hydrothermal mineral assemblage (Angcoy, 2010). The Mahanagdong field discharges low pH fluid with high salinity and has either high or low sulphate concentration. The reservoir fluids with high sulphate acidic fluids have a high concentration of HSO_4 – species that dissociates at lower temperature resulting in an acidic fluid discharge at the wellhead. (Cabahug and Angcoy, 2013)

4. METHODOLOGY

4.1 Data Preparation

4.1.1 Thinning Rate Data

Casing thinning rate can be estimated from the results of a casing inspection caliper (CIC) survey. CIC surveys are conducted with mechanical multi-finger calipers (Figure 1) to check for anomalies in the casing diameter. The mechanical caliper is one of the simplest and most accurate tools for measuring the internal diameter of the casing. It can be used to assess internal corrosion damage, scale build-up, casing collapses, and parted casing breaks.

Figure 1: Photo of a 30-arm Multifinger caliper tool

Surveys in LGPF were conducted using a memory type 30-arm caliper. The tool's 30 feeler arms record the radii of the casing as the distance from the center of the tool to the casing wall. The radii recorded by each arm and the position of each feeler arm are put together to create a representation of the well casing condition. From the 30 radii recorded, the maximum measured inner diameter of the casing was used to represent the minimum thickness of the casing at depth.

Data from the CIC surveys conducted in LGPF two-phase production wells were used to compute for the standardized thinning rate (sTR) of the casings. The thinning rate (TR) of the casing is given by (Equation 1).

$$TR = \left(\frac{pit\ depth}{time}\right) \quad (1)$$

where pit depth is the measured maximum pit depth obtained during the CIC survey. This assumes that observed "pits" in the well are due to material loss and not casing deformation or misalignment. The term *time*, on the other hand, is the estimated amount of time it took for the pits to reach their current state. Since most wells have only been surveyed once, *time* is simply the age of the well.

The thinning rates are normalized against the baseline thicknesses of the casings to get the standardized thinning rate. Since data regarding the casings' original thickness is not readily available, the industry standard for the casing weight is used as a baseline thickness. Table 1 shows the summary of the characteristics of the wells used in this study.

$$sTR = \frac{TR}{casing\ thickness} \quad (2)$$

Table 1. Summary of well characteristics of sample population

No of wells surveyed	19	
	Minimum	**Maximum**
Length of cased hole (m)	739	1948
Casing Diameter (mm)	177.80	339.73
Total Mass flow (kg/s)	5	55
Enthalpy (kJ/kg)	1056	2536

4.1.2 Factors Affecting Corrosion: Fluid Characteristics

For the surveyed wells, only wellhead conditions and fluid chemistry were readily available. Since the surface measurements are known to be different from actual fluid conditions at depth, simulators were used to project the physical and chemical properties down to depth.

The physical properties such as downhole pressure, temperature, fluid velocity, and steam fraction were estimated with the wellbore simulator software HOLA (Björnsson et al., 1993). HOLA calculates the downhole conditions of a flowing well by numerically solving the differential equations that describe the steady-state momentum, energy, and mass conservation equations simultaneously. Boundary conditions for pressure, mass flow and heat content (enthalpy or temperature and steam fraction) are provided to the simulator as either bottom-hole (for "bottom-up" simulations) or wellhead conditions (for "top-down" simulations). In this work, top-down simulations, were done based on measured operating wellhead parameters of the LGPF production wells (Table 2). The top-down simulations were carried out to the production casing shoe to get the pressure and temperature profiles within the casing, which is the region of interest.

Table 2: Fluid discharge data of sample population

Well Name	Date Sampled	WHP (MPag)	MF (kg/s)	H (kJ/kg)	Well Name	Date Sampled	WHP (MPag)	MF (kg/s)	H (kJ/kg)
Well 1	6-May-12	1.10	48.5	1736	Well 11	4-Nov-12	1.3	32.2	1659
Well 2	11-May-11	1.10	4.7	2435	Well 12	26-Feb-11	1.22	29.1	1283
Well 3	4-Nov-10	1.10	36.8	1687	Well 13	13-Sep-11	1.25	42.4	2476
Well 4	8-Dec-11	1.10	28.0	1611	Well 14	26-Nov-12	1.11	30.04	1165
Well 5	27-Nov-10	1.10	24.0	1632	Well 15	20-May-11	1.8	20.9	1482
Well 6	22-Aug-12	1.1	55.2	1056	Well 16	22-Dec-12	1.35	18.86	2413
Well 7	3-Apr-12	1.1	40.6	1085	Well 17	11-Nov-12	1.7	26.4	1325
Well 8	30-Oct-10	1.1	50.6	1315	Well 18	11-Aug-12	1.42-1.55	25.1	2536
Well 9	11-Nov-10	1.1	54.4	1194	Well 19	23-Jul-12	1.2	10.6	2312
Well 10	19-Jun-09	1.1	39.1	1178					

The downhole chemistry of the geothermal fluids as characterized by the pH, and concentrations of Cl, SO_4, H_2S, CO_2 and H_2 were simulated using the software WATCH version 2.4. The Icelandic Water Chemistry Group developed WATCH as a chemical speciation program that could aid in interpreting the chemical composition of geothermal fluids. The program reads the component analyses of water, gas, and steam condensate samples collected at the surface and computes the chemical composition downhole based on chemical equilibria between species at a reference temperature provided by the user. The results provided by WATCH include pH, aqueous speciation, partial pressures of gases, redox potentials, and activity products for mineral dissolution reactions. It was presented to the UN University fellows in 1993. (Arason et al., 2003). Reference temperatures were based on temperature estimates at depth obtained from the HOLA simulation. Figures 2 and 3 show the water and gas chemistry data, respectively, of each well in the sample population; while Table 3 shows the summary of results given by WATCH.

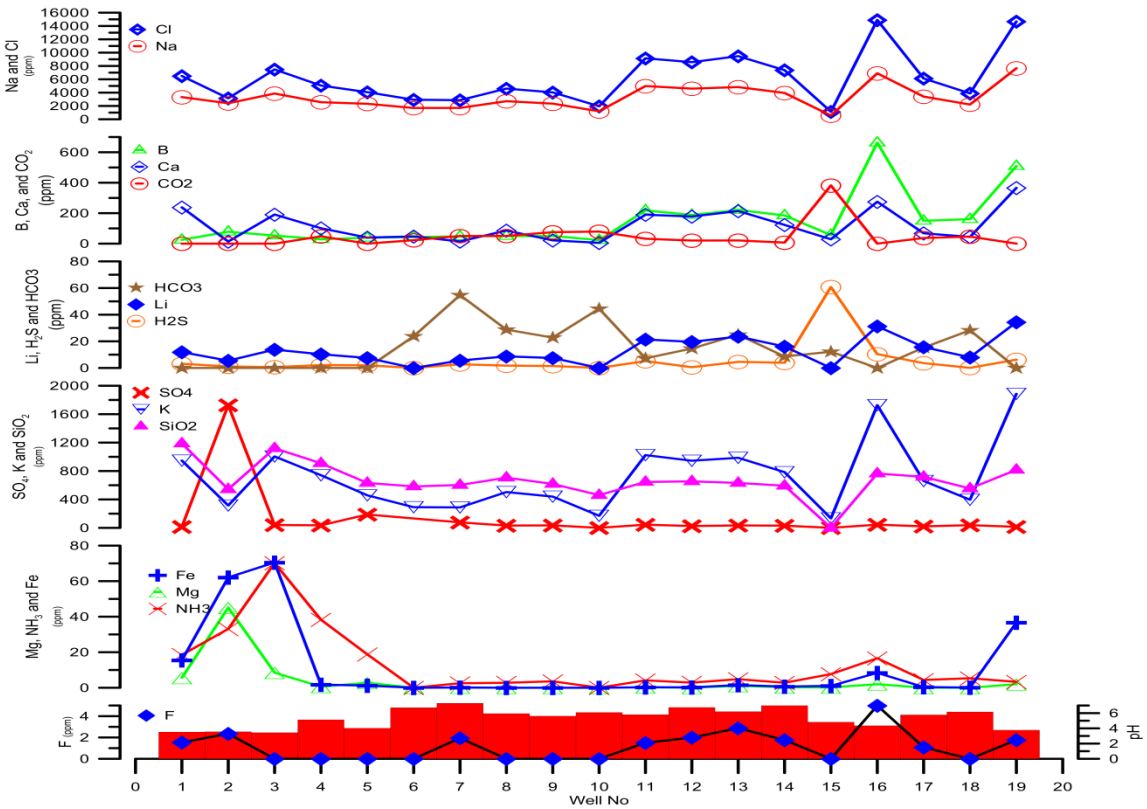

Figure 2. Summary of fluid chemistry data of sample population

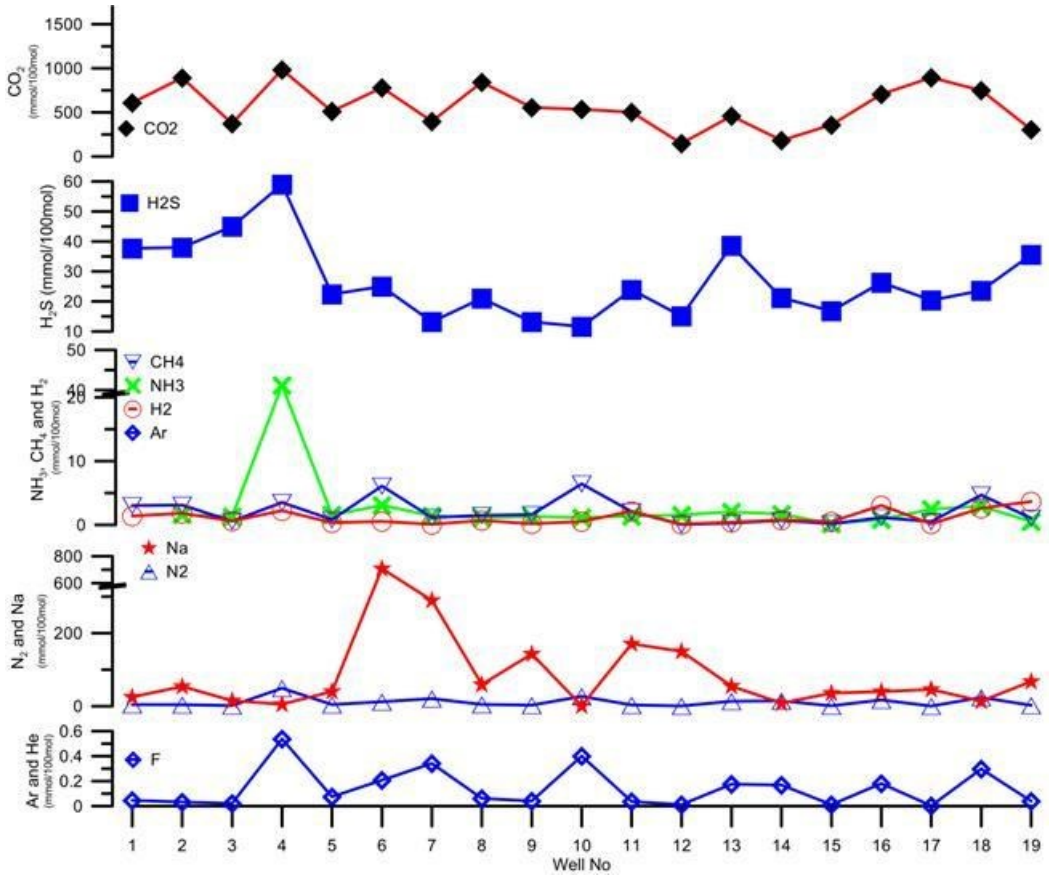

Figure 3. Sampled gas chemistry data of two-phase wells

Table 3. Summary of simulated concentration of corrosion species using software Watch

Range of simulated downhole chemistry of the well studied (ppm)							
Cl_w / 100	SO_{4w} /100	CO_{2w} /100	H_2S_w /100	CO_{2g} /100	H_2S_g /100	H_{2g} /100	Range of fluid pH
9.70 -150.97	0.0 – 17.01	.11 – 12.05	0.02-0.54	35.78 – 560.71	1.76 – 15.34	0.001 -0.0 713	3.6 - 6.9

4.1.3 Factors Affecting Corrosion: Well Characteristics

Well geometry affects the angle of impact of flowing particles on the casing walls. This, in turn, affects how material is lost from the casing walls due to the erosive effect of abrasive particles in the geothermal fluid. The material loss due to erosion is a function of the angle of inclination, θ, which may be obtained using the equation developed by Finnie et al. (1992). For ductile materials, material loss due to erosion is proportional to *f(θ)*, which is given by equations 3 and 4. The angle of inclination of the well was taken from the deviation survey of the well, while the proportionality constant will be calculated during the regression process.

For $\theta \leq 18.5^o$:

$$f(\theta) = (sin\ sin\ 2\theta\ - 3sin^2\theta) \tag{3}$$

And for higher inclinations, $\theta > 18.5^o$

$$f(\theta) = \frac{cos^2\theta}{3} \tag{4}$$

4.2 Development of corrosion model

Regression analysis is a statistical process used for estimating the relationship between variables. Regression analysis seeks to determine the causal effect of one variable upon another and can help in the understanding of how the dependent variable behaves when the independent variables are varied. To understand how the factors affecting the corrosion rate influence the thinning rate of the casing, *sTR* is expressed as a function, F, of the factors affecting the corrosion rates shown in Equations 5 and 6:

$$sTR = F\big(T, V_s, pH, X, f(\theta)\big) \tag{5}$$

$$sTR = F\big(Cl_w, H_2S_w, SO_{4w}, CO_{2w}, H_{2g,}\, H_2S_g, CO_{2g}\big) \tag{6}$$

where sTR = average thinning rate of casing joint (1/year)

T = simulated downhole temperature (°C)

V_s = simulated fluid velocity (m/s)

pH = fluid pH

X = steam fraction

$f(\theta)$ = effect of well inclination

Cl_w = Chloride concentration in water (ppm)

H_2S_w = Hydrogen sulphide in water (ppm)

CO_{2w} = Dissolved Carbon dioxide in water (ppm)

SO_{4w} = Sulphate in water (ppm)

H_2S_g = Hydrogen sulphide gas (ppm)

CO_{2g} = Carbon dioxide gas(ppm)

$H_{2g,}$ = Hydrogen gas (ppm)

D_{ph} = Dummy for fluid pH (D_{ph} = 1 if pH <4.5, else D_{ph} = 0)

D_M = Dummy for Mahanagdong wells (D_M = 1 if wells are from Mahanagdong area, else D_M = 0)

Linear regression with multiple variables was used to develop the function, F. In linear regression, it is assumed that F takes on a linear form or can be transformed to a linear form. If it can be assumed that the different factors affecting corrosion rate affect the casing thinning rate independently, F can take a linear form as shown in Equation 7.

$$sTR \sim \beta_{i-0} + \beta_{i-1}(T) + \beta_{i-2}(V_s) + \beta_{i-3}(pH) + \beta_{i-4}(X) + \beta_{i-5}f(\theta) \quad (7)$$

A multiplicative form of F was based on the mathematical model of flow accelerated corrosion in which factors affecting corrosion rate are interrelated as shown in Equation 8 (Petric and Ksiazek, 1997)

$$WR = F(MT) * F(G) * F(X) * F(pH) * F(O2) * F(T) * F(AC) \quad (8)$$

where WR = Wear rate

$F(MT)$ = Factor for mass transfer effect

$F(G)$ = Factor for geometry effect

$F(X)$ = Factor for void fraction (steam quality)

$F(pH)$ = Factor for pH effect

$F(O_2)$ = Factor for Oxygen effect

$F(T)$ = Factor for temperature effect

$F(AC)$ = Factor for alloy content effect

Equation 8 is a series of products which is transformed to a linear function by taking the logarithm of both sides (Equation 8). The final form of the regression model is given by Equation 9 where A is a proportionality constant.

$$sTR = A * T * V_s * pH * X * f(\theta)$$

$$Log(sTR) = Log(A * T * V_s * pH * X * f(\theta))$$

$$Log(sTR) = Log(A) + Log(T) + Log(V_s) + Log(pH) + Log(X) + Log(f(\theta)) \quad (9)$$

Dummy variables were also used in some of the test models in order to categorize the data into independent groups. In particular, dummy variables were used to differentiate data of acidic wells (pH < 4.5) from data of wells with more neutral fluids and to differentiate Mahanagdong well data from other well data. When a dummy variable for pH was used, concentration of corrosion species was utilized in replacement for the value of the fluid pH in the model. Interactions of the affecting variables with the dummy were used in the regression model to determine which significant species may affect the fluid pH as well as the thinning rate.

The list of cases for the regression analysis are summarized in Table 4.

Table 4. Regression equations for predicting casing thinning rate from factors affecting corrosion rate

Case	Regression Model
1	$log\ (sTR) \sim \beta_{1-0} + \beta_{1-1} log\ (T) + \beta_{1-2} log\ (pH) + \beta_{1-3} log\ (X) + \beta_{1-4} log\ (V_s) + \beta_{1-5} log\ (f(\theta))$
2	$sTR \sim \beta_{2-0} + \beta_{2-1}(Cl_w) + \beta_{2-2}(SO_{4_w}) + \beta_{2-3}(CO_{2_w}) + \beta_{2-4}(H_2S_w) + \beta_{2-5}(CO_{2_g}) + \beta_{2-6}(H_2S_g) + \beta_{2-7}(H_{2_g})$
3	$log\ (sTR) \sim \beta_{3-0} + \beta_{3-1} log\ (CO_{2_w}) + \beta_{3-2} log(Cl_w) + \beta_{3-3} log(SO_{4_w}) + \beta_{3-4} log(H_2S_w) + \beta_{3-5} log(CO_{2_g}) + \beta_{3-6} log(H_2S_g) + \beta_{3-7} log(H_{2_g})$
4	$log\ (sTR) \sim \beta_{4-0} + \beta_{4-1} log\ (T) + \beta_{4-2} log\ (X) + \beta_{4-3} log\ (V_s) + \beta_{4-4} log\ (f(\theta)) + D_{pH}[\beta_{4-5} + \beta_{4-6} log\ (T) + \beta_{4-7} log\ (X) + \beta_{4-8} log\ (V_s) + \beta_{4-9} log\ (f(\theta))\ ]$
5	$log\ (sTR) \sim \beta_{5-0} + \beta_{5-1}\ log\ (T) + \beta_{5-2}\ log\ (X) + \beta_{5-3}\ log\ (V_s) + \beta_{5-4}\ log\ (f(\theta)) + \beta_{5-5} D_{pH} + \beta_{5-6}\ log\ (CO_{2_w}) + \beta_{5-7}\ log\ (Cl_w) + \beta_{5-8}\ log\ (SO_{4_w}) + \beta_{5-9}\ log\ (CO_{2_g}) + \beta_{5-10}\ log\ (H_2S_g) + \beta_{5-11}\ log\ (H_{2_g}) + D_{pH}[\beta_{5-12}\ log\ (T) + \beta_{5-13}\ log\ (X) + \beta_{5-14}\ log\ (V_s) + \beta_{5-15}\ log\ (f(\theta))\ ]$
6	$log\ (sTR) \sim \beta_{6-0} + \beta_{6-1}\ log\ (T) + \beta_{6-2}\ log\ (X) + \beta_{6-3}\ log\ (V_s) + \beta_{6-4}\ log\ (f(\theta)) + \beta_{6-6}\ log\ (CO_{2_w}) + \beta_{6-9}\ log\ (SO_{4_w}) + \beta_{6-12}\ log\ (CO_{2_g}) + \beta_{6-14}\ log\ (H_2S_g) + \beta_{6-16}\ log\ (H_{2_g}) + D_{pH}\left[\beta_{6-5} + \beta_{6-7}\ log\ (CO_{2_w}) + \beta_{6-8}\ log\ (Cl_w) + \beta_{6-10}\ log\ (SO_{4_w}) + \beta_{6-11}\ log\ (H_2S_w) + \beta_{6-13}\ log\ (CO_{2_g}) + \beta_{6-15}\ log\ (H_2S_g) + \beta_{6-17}\ log\ (H_{2_g}) + \beta_{6-18}\ log\ (T) + \beta_{6-19}\ log\ (X) + \beta_{6-20}\ log\ (V_s) + \beta_{6-21}\ log\ (f(\theta))\right]$
7	$log\ (sTR) \sim \beta_{7-0} + \beta_{7-1}\ log\ (T) + \beta_{7-2}\ log\ (X) + \beta_{7-3}\ log\ (V_s) + \beta_{7-4}\ log\ (f(\theta)) + \beta_{7-6}\ log\ (Cl_w) + \beta_{7-8}\ log\ (SO_{4_w}) + \beta_{7-10}\ log\ (CO_{2_w}) + \beta_{7-12}\ log\ (H_2S_w) + \beta_{7-14}\ log\ (CO_{2_g}) + \beta_{7-16}\ log\ (H_2S_g) + \beta_{7-18}\ log\ (H_{2_g}) + D_{pH}\left[\beta_{7-5} + \beta_{7-7}\ log\ (Cl_w) + \beta_{7-9}\ log\ (SO_{4_w}) + \beta_{7-11}\ log\ (CO_{2_w}) + \beta_{7-13}\ log\ (H_2S_w) + \beta_{7-15}\ log\ (CO_{2_g}) + \beta_{7-17}\ log\ (H_2S_g) + \beta_{7-19}\ log\ (H_{2_g}) + \beta_{7-20}\ log\ (T) + \beta_{7-21}\ log\ (X) + \beta_{7-22}\ log\ (V_s) + \beta_{7-23}\ log\ (f(\theta))\right]$
8	$log\ (sTR) \sim \beta_{8-0} + \beta_{8-1}\ log\ (X) + \beta_{8-2}\ log\ (V_s) + \beta_{8-3}\ log\ (f(\theta)) + \beta_{8-5}(SO_{4_w}) + \beta_{8-6}(CO_{2_w}) + \beta_{8-7}(CO_{2_g}) + \beta_{8-8}(H_{2_g}) + \beta_{8-9}(H_2S_g) + \beta_{8-10}(Cl_w) + D_{pH}\left[\beta_{8-4} + \beta_{8-11}(Cl_w) + \beta_{8-12}(CO_{2_g})\right]$
9	$log\ (sTR) \sim \beta_{9-0} + \beta_{9-1}\ log\ (X) + \beta_{9-2}\ log\ (V_s) + \beta_{9-3}\ log\ (f(\theta)) + \beta_{9-5}(SO_{4_w}) + \beta_{9-6}(CO_{2_w}) + \beta_{9-7}(CO_{2_g}) + \beta_{9-8}(H_{2_g}) + \beta_{9-9}(H_2S_g) + \beta_{9-11}(Cl_w) + D_{pH}\left[\beta_{9-4} + \beta_{9-9}(H_2S_g) + \beta_{9-12}(Cl_w) + \beta_{9-13}(CO_{2_g})\right]$

10	$log\ (sTR) \sim \beta_{10-0} + \beta_{10-1}\ log\ (X)\ + \beta_{10-2}\ log\ (V_s)\ + \beta_{10-3}\ log\ (f(\theta))\ + \beta_{10-5}(SO_{4_w}) + \beta_{10-6}(CO_{2_w}) + \beta_{10-7}\left(CO_{2_g}\right) + \beta_{10-8}\left(H_{2_g}\right) + \beta_{10-9}(H_2S_g) + \beta_{10-10}(Cl_w) + D_{pH}\left[\beta_{10-4} + \beta_{10-12}(H_2S_g) + \beta_{10-13}(Cl_w) + \beta_{10-14}\left(CO_{2_g}\right)\right] + D_M\left[\beta_{10-11} + \beta_{10-15}(H_2S_g) + \beta_{10-16}(Cl_w) + \beta_{10-17}\left(CO_{2_g}\right)\right]$
11	$log\ (sTR) \sim \beta_{11-0} + \beta_{11-1}\ log\ (X)\ + \beta_{11-2}\ log\ (T)\ + \beta_{11-3}\ log\ (V_s)\ + \beta_{11-4}\ log\ (f(\theta)) + \beta_{11-7}(SO_{4_w}) + \beta_{11-8}\left(CO_{2_g}\right) + \beta_{11-9}\left(H_{2_g}\right) + \beta_{11-10}(H_2S_g) + \beta_{10-10}(Cl_w) + D_{pH}\left[\beta_{11-5} + \beta_{11-11}log(X) + \beta_{11-12}(SO_{4_w})\right] + D_M\left[\beta_{11-6} + \beta_{11-13}\left(CO_{2_g}\right) + \beta_{11-14}\left(H_{2_g}\right) + \beta_{11-15}(H_2S_g)\right]$

where β_{i-0} and β_{i-k} are the normal and slope coefficients due to the affecting factors and corrosion species$\left(T, V_s, pH, X, f(\theta), Cl_w, H_2S_w, SO_{4w}, CO_{2w}, H_{2g,}\ H_2S_g, CO_{2g}, D_{pH}, D_M\right)$.

The multiple regression and analysis of variance (ANOVA) test was performed at a 95% confidence level in order to examine the combined effects of temperature, fluid velocity, fluid pH, well geometry, steam fraction, and corrosion species such as chloride, sulphate, hydrogen, carbon dioxide and hydrogen sulphide on thinning rate of the geothermal well casing.

4.3 Selection of a good model

Two criteria were used to select good models for predicting the casing thinning rate. The first criterion is the adjusted coefficient of determination (R_a^2) and the second is the mean absolute percentage error (MAPE).

R_a^2, is a variation of the coefficient of determination, R^2, which is proportional to the variation of the response variable.

$$R_a^2 = \left(\frac{MS_{Tot} - MS_{error}}{MS_{Tot}}\right) \tag{10}$$

where MS = Mean of squares

This kind of variation or R^2 includes a penalty for the unnecessary explanatory variables. It measures the proportion of the observed spread in the responses that as explained by the model. The higher value of adjusted R^2 illustrates a good correlation.

Another set of criteria used in selecting the model is the mean absolute percentage error (MAPE). It is a measure of accuracy of a method for constructing fitted values in statistics specifically for estimation. MAPE is expressed as a percentage as shown in equation 11. The model with lower MAPE is a good prediction model.

$$MAPE = \frac{1}{n}\sum_{i}^{n} \left|\frac{Actual_i - Predicted_i}{Actual_i}\right| \tag{11}$$

5. RESULTS AND DISCUSSION

The correlation results of the standardized thinning rate of the casing as a dependent variable, and the factors affecting it $(T, V_s, pH, X, f(\theta),)$ are summarized in Table 5. Some of the case models were reduced which maintains only the significant variables affecting the standardized thinning rate.

The coefficient of determination adjusted R^2 ranges from 0.442 to 0.690 for cases 1 to 9. This can be interpreted as 44% to 69% of the standardized thinning rate and may be explained by the factors affecting corrosion rate considered during the regression. Regression analysis with a categorical dummy variable for Mahanagdong wells increases the adjusted R^2 from 0.6993 to 0.7054 based on the results of Case 10 to 11.

The MAPEs of the regression models are also shown in Table 5. Among the 11 case models, case 11 appears to be the best model because it has the highest adjusted R^2 and the lowest MAPE.

Table 5. Correlation results of the thinning rate in the casing and Mean absolute percentage error (MAPE)

Case Model	Multiple R^2	Adjusted R^2	Residual Standard Error	Observation	MAPE
1	0.5496	0.5477	0.8759	1188	173.5357
2	0.5767	0.5741	1.648	1188	227.4201
2 (Reduced form)	0.5764	0.5746	1.647	1188	226.9901
3	0.4453	0.442	0.9729	1188	153.4524
4	0.6106	0.6076	0.8159	1188	116.9374
4 (Reduced form)	0.5807	0.5785	0.8456	1188	123.6762
5	0.6723	0.6678	0.7506	1188	103.1594
5 (Reduced form)	0.6396	0.6375	0.7842	1188	106.5819
6	0.6808	0.6745	0.743	1188	100.0671
6 (Reduced form)	0.6344	0.6326	0.7895	1188	105.6735
7	0.7059	0.7001	0.7132	1188	93.2827
7 (Reduced form)	0.685	0.6821	0.7344	1188	102.0898
8	0.6877	0.6845	0.7316	1188	100.3288
9	0.6935	0.6901	0.725	1188	98.92965
10	0.706	0.7017	0.7114	1188	98.483
10 (Reduced form)	0.7021	0.6993	0.7142	1188	101.758
11	0.7091	0.7054	0.707	1188	95.89386

The low values of the coefficient of determination may be due to the effect of the other factors not considered in the models, such as the condition of the casing joints used in a geothermal well. It is possible that the casing already had corrosion pits before it was installed in the borehole. Well stimulation and other well intervention operations conducted on the well like workovers could also significantly affect the condition of the casing. During workovers, particularly in mechanical clearing operations, the inner walls of the casing is stressed by the drill bit. Casing joints located at sections with high deviation are the most affected by the drill pipes.

Consistent with the low R^2 values, the residuals, as measured by the MAPE, are high. The large MAPE's may partially be a result of the log-transformations applied on the results. Transformation may bias the results as residuals become the exponent of a scaling factor. This is of little consequence when residuals are close to 0, but when they are considerable, the scaling factor becomes much greater than 1.

The parameter estimates of the case 11 model is shown in Table 6 and were analyzed. Based from the parameter estimates, dummy variable D_{pH} has high value of coefficient which illustrates that wells with low pH has a high thinning rate of the casing. This suggests that the pH of the fluid is a dominant controlling factor of the thinning rate of the casing. This statistical finding is in agreement with the experimental results of Sanada et al., (1998), which states that the pH of the fluid dominantly controls the corrosion rate.

Among the corrosion species, the concentrations of SO_{4w}, CO_{2g}, H_{2g} and H_2S_g were found to be significant in the model in predicting the thinning rate of the casing.

The factors affecting the thinning rate of the two-phase wells such as the fluid velocity have negative coefficients indicating a decreased effect on the thinning rate as the fluid velocity increased. The velocity of the fluid at downhole increases as the fluid phase changes from single to two-phase as induced by boiling. This implies that thinning of the casing occurs at the velocity were the fluid is in the liquid phase condition. Slow velocity of the fluid results in a longer residence time and more time for thinning reaction at the surface of the casing to happen.

Table 6. Summary of parameter estimate of Case Model 11

Case Model 11					
Variables		*Coefficients*	*Standard Error*	*t Stat*	*P-value*
Intercept	β_{11-0}	-5.4165798	3.228912	-1.678	0.093707
Log (X)	β_{11-1}	0.0793396	0.126981	0.625	0.532214
Log (T)	β_{11-2}	1.1755113	0.599236	1.962	0.050036
Log (V_s)	β_{11-3}	-0.48012	0.111198	-4.318	1.71E-05
Log (f(θ))	β_{11-4}	0.0490647	0.007627	6.433	1.82E-10
D_{pH}	β_{11-5}	-7.7400337	1.887446	-4.101	4.40E-05
D_M	β_{11-6}	0.5358158	0.192215	2.788	0.005396
SO_{4w}	β_{11-7}	0.0675302	0.018318	3.687	0.000238
CO_{2g}	β_{11-8}	0.0046766	0.000901	5.188	2.50E-07
H_{2g}	β_{11-9}	-1.5777953	3.298903	-0.478	0.632541
H_2S_g	β_{11-10}	-0.1016067	0.029346	-3.462	0.000555
Log (X)* D_{pH}	β_{11-11}	2.1300475	0.41068	5.187	2.52E-07
(SO_{4w}) * D_{pH}	β_{11-12}	8.0572391	2.350282	3.428	0.000629
(CO_{2g})* D_M	β_{11-13}	-0.0120913	0.001325	-9.126	< 2e-16
(H_{2g})* D_M	β_{11-14}	90.432761	12.59875	7.178	1.25E-12
(H_2S_g)* D_M	β_{11-15}	0.1273445	0.039853	3.195	0.001434

The increase in steam fraction, temperature, and well inclination corresponds to an increase in the thinning rate of the casing as interpreted from the coefficient of the parameter estimates as shown in Table 6. The result of the regression of the steam fraction shows that the thinning rate of the casing increases with increased steam fractions. When the geothermal fluid flashes inside the wellbore, it changes from single phase to two-phase fluid which results in an increase of steam component. The flashing of the geothermal brine changes the concentration of the dissolved gases and these would probably result in decreases in pH from the well studied.

Temperature effect on thinning rate is directly proportional to the thinning rate, based on the selected regression model. The result of the regression model agrees to the study of Sanada (1998) wherein the experiment with different casing types exposed in different temperature ranges from 105 C to 137 C with different fluid pH, corrosion rates are significantly dependent on temperature, particularly when fluid pH is low.

Based on the regression analysis, the deviated well geometry shows an increase effect in thinning rate. However, the contribution of this factor to the thinning rate is very low compared to other factors. A deviated well geometry will cause more turbulence in fluid flow. Corrosion rate is much higher for a turbulent flow having a low pH concentration (Sanada et al., 1998).

These variables are in log transformed as well as the standardized thinning rate. Interpreting the effect of temperature to the thinning rate based from the parameter estimate would mean an increase of one percent in the temperature would result in a change of 1.17% increase in the standardized thinning rate while all other variables in the model are held constant.

Parameter estimate of the dummy variable D_M were analyzed in the regression model. It shows that wells in Mahanagdong area have high thinning rate compared to non-Mahanagdong wells due to its positive coefficient which will be added to the intercept (β_{11-0}).

The coefficients of the parameter estimate listed in Tables 9 were used for developing the set of linear regression equations for standardized thinning rates of geothermal casing. Equations 12 to 15 are the simplified regression model established for the wells in Mahanagdong with low and neutral pH and for non-Mahanagdong with low and neutral pH.

For Mahanagdong wells ($D_M = 1$) with pH < 4.5 ($D_{pH} = 1$)

$$\text{Log (sTR)} \sim -12.621 + (2.209)*\text{Log(X)} + (1.176)*\text{Log(T)} + (-0.480)*\text{Log}(V_s) + (0.049)*\text{Log}(f(\theta)) + (8.125)*(SO_{4w}) + (-0.007)*(CO_{2g}) + (88.855)*(H_{2g}) + (0.025)*(H_2S_g) \quad (12)$$

For Mahanagdong wells ($D_M = 1$) with pH > 4.5 ($D_{pH} = 0$)

$$\text{Log (sTR)} \sim -4.881 + (0.079)*\text{Log(X)} + (1.176)*\text{Log(T)} + (-0.480)*\text{Log}(V_s) + (0.049)*\text{Log}(f(\theta)) + (0.068)*(SO_{4w}) + (-0.007)*(CO_{2g}) + (88.855)*(H_{2g}) + (0.025)*(H_2S_g) \quad (13)$$

For Non-Mahanagdong wells ($D_M = 0$) with pH < 4.5 ($D_{pH} = 1$)

$$\text{Log (sTR)} \sim -12.621 + (2.209)*\text{Log(X)} + (1.176)*\text{Log(T)} + (-0.480)*\text{Log}(V_s) + (0.049)*\text{Log}(f(\theta)) + (8.125)*(SO_{4w}) + (0.005)*(CO_{2g}) + (-1.578)*(H_{2g}) + (-0.102)*(H_2S_g) \quad (14)$$

For Non-Mahanagdong wells ($D_M = 0$) with pH > 4.5 ($D_{pH} = 0$)

$$\text{Log (sTR)} \sim -5.417 + (0.079)*\text{Log(X)} + (1.176)*\text{Log(T)} + (-0.480)*\text{Log}(V_s) + (0.049)*\text{Log}(f(\theta)) + (0.068)*(SO_{4w}) + (0.005)*(CO_{2g}) + (-1.578)*(H_{2g}) + (-0.102)*(H_2S_g) \quad (15)$$

Based from the simplified equation, wells with low pH have high parameter estimates of SO4w compared to wells with neutral pH. This could illustrate that fluid pH of wells studied were controlled by the concentration of HSO4 as also observed in Mahanagdong Sector that reservoir fluids with high sulphate acidic fluids have a high concentration of the HSO4 species that dissociates at a lower temperature, resulting in an acidic fluid discharge at the wellhead (Cabahug and Angcoy, 2013). Interpreting the effect of the corrosion species in relation to the standardized thinning rate is different than the interpretation of the coefficient for the temperature and other affecting factors, since thinning rate is at log transform and corrosion species are not. In such case, the thinning rate would mean an increase of 6.8% for every one percent increase of SO_{4w} while all other variables in the equation 15 are held constant for non-Mahanagdong wells with low pH.

Parameter estimate of the regression model of case 11 model shows that for the studied wells, species of H_2S gas and H_{2g} significantly contribute to the thinning rate of the casing of Mahanagdong wells. The casing used in most of the geothermal wells are carbon steel K55. This type of casing has a small percentage of copper and nickel; and when hydrogen sulphides are present, the corrosion is severe. High concentrations of H_2 gas in the well shows a high correlation to an increased thinning rate of the casing. Increased hydrogen concentration lowers the pH of the fluid. The casing experiences stress corrosion cracking at higher concentrations of hydrogen gas. On the other hand, low concentration of hydrogen gas in the well results in the formation of scales which protects the casing from the corrosive fluid and slows down the corrosion of the casing. Metals become brittle because of the absorption and diffusion of hydrogen at the molecular level. The embrittlement is much more severe when hydrogen sulphide is present (Prasetia et al., 2010)

Figures 4 show the plot of the observed thinning rate of the casing and the fitted value of the thinning using the factors affecting and corrosive species for the two-phase wells. The sample of data are plotted and categorized as low pH and neutral pH as well as data that are located in and out of the Mahanagdong area. It is shown in the plots that observed thinning rates of two-phase wells are scattered for wells with low pH fluid. However categorizing the model into Mahanagdong wells to non-Mahanagdong wells and utilizing corrosion species with the other factors for the model case 11, the fitted value was improved against the observed values base.

A repeat of the caliper surveys for Well 2, 11 and 15 were used to compare the predicted thinning rate using case models 11. The average casing thinning rate of the repeated survey was compared to the average predicted thinning rate of the casing.

The predicted thinning rate of the caliper survey were found to be an underestimate by case model 11 for Well 1 while being an overestimate for Well 15 and Well 2 as shown from Figure 5. Well 1 and Well 2 have large differences between the measured and the predicted average thinning rate of the casing. This was expected since the predicted values of the regression do not match the observed value in the regression model plot.

Comparing the first and second surveys, the trend on the change of thinning rates for the three wells between first and second caliper surveys shows similar trend on the predicted thinning rates of the casing using the case 11 models as shown in Figure 6. Even the average predicted thinning rate of the case model does not match the observed average thinning rate from the caliper survey. Despite this, the model can still be used as a tool to determine the candidate wells to be surveyed. By knowing the trend of the thinning rate of the casing based from the results of the prediction model, wells with a high risk for corrosion should be monitored more frequently. Moreover corrosion mitigating actions should be performed on these wells in order to prevent the high risk associated with the utilization of these wells.

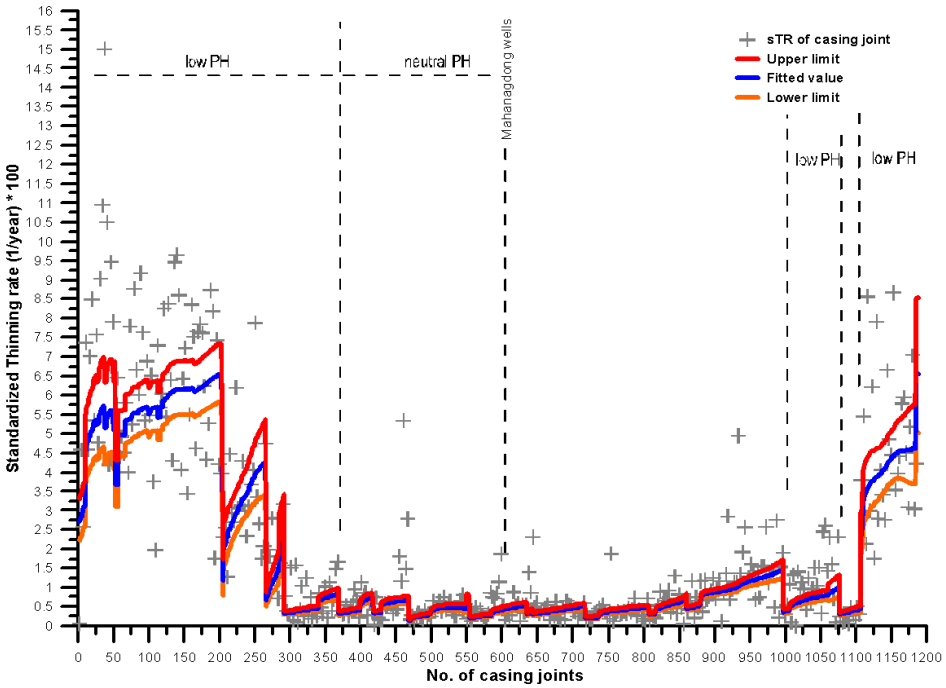

Figure 4. Plot of observed and predicted thinning rate using case 11 model

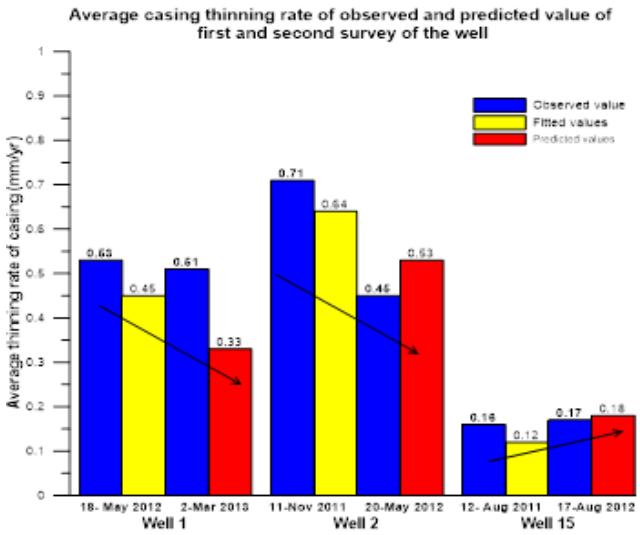

Figure 5. Bar chart of average casing thinning rate of measured second caliper survey and average predicted thinning rate of wells Well 1, Well 2 and Well 15 using case 11 model

Figures 6 to 8 show the actual and predicted sTR and thinning rate (TR) of the repeated surveys for Well 15, Well 2 and Well 1. Thinning rates (TR) are computed by multiplying the sTR by the thickness of the casing joint. It is observed that most of the predicted thinning rate in well Well 15 and Well 2 are above to the actual TR of the well which reflects the overestimated average thinning rate as shown in Figure 5. The predicted thinning rate of Well 1 is observed below the actual TR of the casing joint showing an underestimate of the prediction.

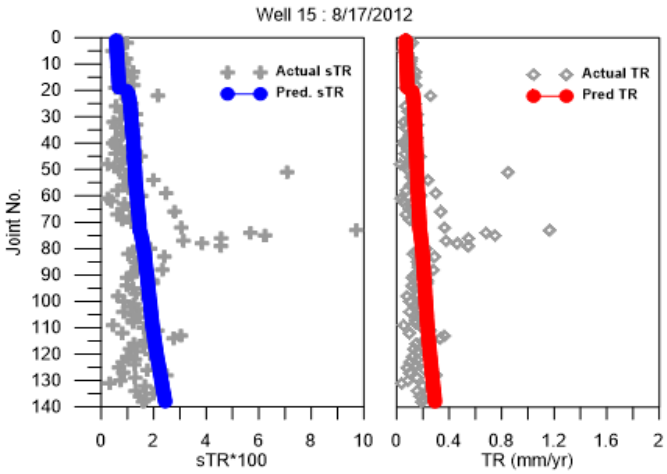

Figure 6. Plot of actual and predicted sTR and TR of Well 15 using case 11 model

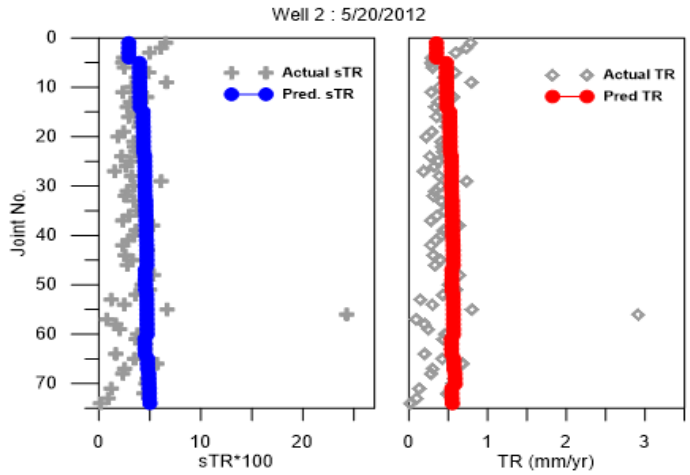

Figure 7. Plot of actual and predicted sTR and TR of well Well 2 using case 11 model

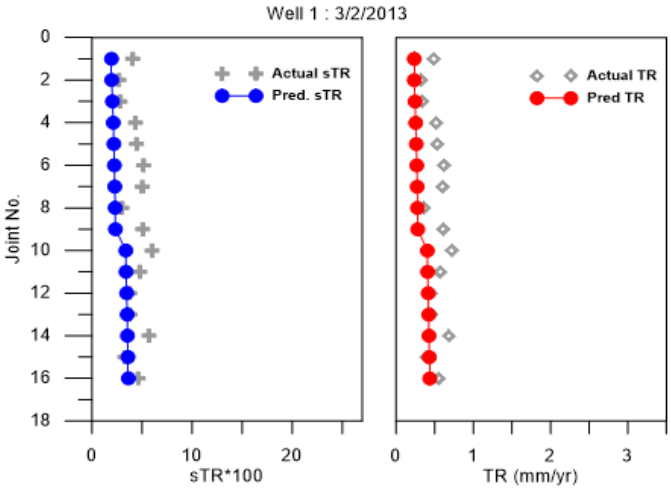

Figure 8. Plot of actual and predicted sTR and TR of well Well 1 using case 11 model

6. SUMMARY AND CONCLUSIONS

Monitoring the thinning rate of the geothermal well casing is essential in managing the geothermal production field. The loss of integrity of the casing due to thinning could result in a high risk in operations safety, environmental damage and loss of profit. Exposure to geothermal fluid is the main cause of thinning of the casing.

Regression modelling was used in the study of thinning rates of geothermal casings of Leyte Geothermal Production Field. Using the software HOLA and WATCH, downhole conditions were projected from fluid discharge measurements and fluid sample chemistry at the wellhead. The simulated data were used as datasets for the regression model of the thinning rate of the casing. The results of caliper inspection surveys, conducted on the well casing, were used as the response variable to the regression model.

The regression analysis showed that fluid discharge characteristics such as temperature, velocity, steam fraction and geometry of the well combined with the corrosion species are highly significant to the thinning rate of the geothermal casing for the two-phase wells. These factors contribute 44.2% to 70.5% to the thinning of the casing. The use of dummy variables such as D_{pH} and D_M used in the regression model to categorize casing joints with low pH and belongs to well in Mahanagdong area have improved the model in fitting the actual data.

Even the model has been improved from base case 1. The model was found to be inadequate for accurately predicting the thinning of the casing. Other factors or statistical methods need to be considered in the model in order to improve the reliability of the model for predicting the casing thickness in the case of the dry wells.

The regression model needs further refinement before it can provide accurate prediction of the casing-thinning rate. The model was used on low pH wells and it is recommended to test the model on high pH wells in order to validate the model further and to test its reliability in predicting the thinning rate of the casing. In the meantime, the model may be used to determine if casing thinning rate is increasing or decreasing which can be used as a criteria for selecting wells for casing inspection.

The low coefficient of determination (adjusted R^2) of the regression model could be attributed to the condition of the casing before it was installed in the borehole. The well stimulation activities conducted on some of the wells included in this study have a significant bearing on the result of the regression modelling.

REFERENCES

Angcoy, E. and Arnórsson S, 2010: Geochemical modelling of the high-temperature Mahanagdong geothermal field, Leyte, Philippines. University of Iceland, MSc thesis, UNU-GTP, report 1, 79 pp.

Arason, Th., Björnsson, G., Axelsson, G., Bjarnason, J.Ö., and Helgason, P., 2003: The geothermal reservoir engineering software package ICEBOX, user´s manual. Orkustofnun, Reykjavík, report, 48 pp.

Bjarnason, J.Ö. (1994), "The speciation program WATCH, version 2.1," Orkustofnun, Reykjavík, 7 pp.

Björnsson, G., Arason, P., Bödvarsson, G.S., 1993: The wellbore simulator HOLA. Version 3.1. User's guide. Orkustofnun, Reykjavík, 3 pp.

Cabahug, M.R.S., and Angcoy, E.C.Jr, 2013: Modeling the reservoir fluids of acidic geothermal wells in Mahanagdong, Leyte, Philippines. *Procedia Earth & Planetary Science, 7,* 105-108.

Finnie, I., Stevick, G.R. and Ridgely, J.R., 1992: The influence of impingement angle on the erosion of ductile metals by angular abrasive particles. Wear, 152, 91-98.

Elguedri, M., 1999: Assessment of scaling and corrosion problems in the Kebili geothermal field, Tunisia. Report 1 in: Geothermal Training in Iceland 1999. UNU-GTP, Iceland, 1-40.

Petric, G., and Ksiazek, P., 1997: Flow-accelerated corrosion in industrial steam and power plants. Proceedings of the Engineering & Papermakers Conference 1997, 1537-1542.

Prasetia, A.E., Salazar A.T.N. and Toralde, J.S.S., 2010: Corrosion control in geothermal aerated fluids drilling projects in Asia Pacific. Proceedings of the World Geothermal Congress 2010, Bali, Indonesia, 7 pp.

Sanada, N., Kurata, Y., Nanjo, H., Ikeuchi, J. and Kimura, S., 1998: Corrosion in acidic geothermal flows with high velocity. Proceedings of the 20th New Zealand Geothermal Workshop, 121-126